

MambaVision: A Hybrid Mamba-Transformer Vision Backbone

Ali Hatamizadeh, Jan Kautz
 NVIDIA
 {ahatamizadeh, jkautz}@nvidia.com

Abstract

We propose a novel hybrid Mamba-Transformer backbone, denoted as MambaVision, which is specifically tailored for vision applications. Our core contribution includes redesigning the Mamba formulation to enhance its capability for efficient modeling of visual features. In addition, we conduct a comprehensive ablation study on the feasibility of integrating Vision Transformers (ViT) with Mamba. Our results demonstrate that equipping the Mamba architecture with several self-attention blocks at the final layers greatly improves the modeling capacity to capture long-range spatial dependencies. Based on our findings, we introduce a family of MambaVision models with a hierarchical architecture to meet various design criteria. For Image classification on ImageNet-1K dataset, MambaVision model variants achieve a new State-of-the-Art (SOTA) performance in terms of Top-1 accuracy and image throughput. In downstream tasks such as object detection, instance segmentation and semantic segmentation on MS COCO and ADE20K datasets, MambaVision outperforms comparably-sized backbones and demonstrates more favorable performance. Code: <https://github.com/NVlabs/MambaVision>.

1 Introduction

During the recent years, Transformers [1] have become the de facto architecture in different domains including in computer vision, natural language processing, speech processing and robotics. In addition, the versatility of the Transformer architecture, primarily due to its attention mechanism, and its flexibility makes it highly suitable for multimodal learning tasks, where integrating and processing information from various modalities is essential. Despite these benefits, the quadratic complexity of the attention mechanism with respect to sequence length make Transformers computationally expensive to train and deploy. Recently, Mamba [2] proposed a new State Space Model (SSM) that achieves linear time complexity and outperforms or matches Transformers in different language modeling tasks [2]. The core contribution of Mamba is a novel selection mechanism that enables efficient input-dependent processing of long sequences with hardware-aware considerations.

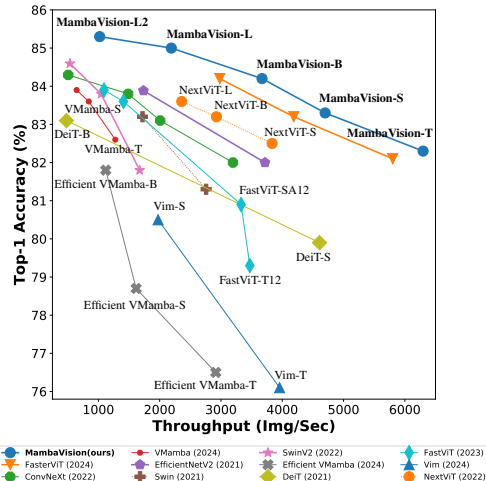


Figure 1 – Top-1 accuracy vs. image throughput on ImageNet-1K. All measurements conducted on A100 GPU with batch size of 128. MambaVision achieves a new SOTA Pareto front.

Recently, a number of Mamba-based backbones [3, 4] have also been proposed to leverage the strengths of its SSM formulation in vision tasks such as image classification and semantic segmenta-

tion. However, the Mamba’s autoregressive formulation, while effective for tasks requiring sequential data processing, faces limitations in computer vision tasks that benefit from a full receptive field: (1) Unlike sequences where order matters, image pixels do not have a sequential dependency in the same way. Instead, spatial relationships are often local and need to be considered in a more parallel and integrated manner. Hence, this results in inefficiency for processing spatial data (2) an autoregressive model like Mamba processes data step-by-step, limiting its ability to capture and utilize global context in one forward pass. In contrast, vision tasks often require understanding the global context to make accurate predictions about local regions.

Vision Mamba (Vim) [3] and others have proposed modifications such as bidirectional SSMS to address lack of global context and spatial understanding. While bidirectional SSMS have the potential to capture more comprehensive context, they introduce significant latency due to the need to process the entire sequence before making predictions. Additionally, the increased complexity can lead to challenges in training, risk of overfitting, and may not always result in better accuracy. Due to these pitfalls, backbones with Vision Transformer (ViT) and Convolutional Neural Network (CNN) architectures still outperform best Mamba-based vision models on different vision tasks.

In this work, we systematically re-design the Mamba block to make it more suitable for vision tasks. We propose a hybrid architecture that consists of our proposed formulation (*i.e.* MambaVision Mixer and MLP) as well as Transformer blocks. Specifically, we study different integration patterns such as adding the Transformer blocks in an iso-parameter manner to earlier, middle and final layers as well as every l layers. Our analysis shows that leveraging several self-attention blocks at the final stages can significantly enhance the capability to capture global context and long-range spatial dependencies. As shown in Sec. 5, using a hybrid architecture also results in a higher image throughput in comparison to both pure Mamba or ViT-based models.

We introduce the MambaVision model which consists of a multi-resolution architecture and leverages CNN-based residual blocks for fast feature extraction of larger resolution features. As shown in Fig. 1, the MambaVision achieves a new SOTA Pareto front in terms of ImageNet-1K Top-1 accuracy and image throughput, outperforming Mamba, CNN and ViT-based models, sometimes by a significant margin. In downstream tasks such as Object detection and instance segmentation as well as semantic segmentation, models with MambaVision backbones outperform comparably-sized counterparts on MS COCO and ADE20 datasets, respectively. Hence, it validates the effectiveness and versatility of MambaVision as an efficient backbone.

To the best of our knowledge, MambaVision is the *first* effort to study and develop a hybrid architecture comprising of both Mamba and Transformers for computer vision applications. Our main contributions in this work are summarized as follows:

- We introduce a redesigned vision-friendly Mamba block, improving accuracy and image throughput over the original Mamba architecture.
- We present a systematic investigation of integration patterns for Mamba and Transformer blocks and demonstrate that incorporating self-attention blocks at the final stages significantly improves the model’s ability to capture global context and long-range spatial dependencies.
- We introduce MambaVision which is a novel hybrid Mamba Transformer model. The hierarchical MambaVision achieves a new SOTA Pareto front on ImageNet-1K dataset in terms of Top-1 and image throughput tradeoff.

2 Related work

ViT. The Vision Transformer (ViT) [5] emerged as a promising alternative to CNNs, leveraging self-attention layers to provide an enlarged receptive field. However, ViTs initially lacked some of the inherent advantages of CNNs, such as inductive biases and translation invariance, and they required large-scale training datasets to achieve competitive performance. To address these limitations, the Data-efficient Image Transformer (DeiT) [6] introduced a distillation-based training strategy that significantly improved classification accuracy, even with smaller datasets. Building on this, the LeViT [7] model proposed a hybrid approach, incorporating redesigned MLP and self-attention modules optimized for fast inference, enhancing both efficiency and performance. Furthermore, the Cross-covariance Image Transformer (XCiT) [8] introduced a transposed self-attention mechanism, effectively modeling interactions between feature channels and improving the model’s ability to cap-

ture complex patterns in the data. The Pyramid Vision Transformer (PVT) [9] adopted a hierarchical structure with patch embedding at the start of each stage and spatial dimension reduction, thereby improving computational efficiency. Similarly, Swin Transformers [10] proposed a layered architecture where self-attention is computed within local windows, which are shifted to enable interaction between regions, balancing local and global contexts. The Twins Transformer [11] featured spatially separable self-attention that significantly enhanced efficiency. In addition, the Focal Transformer [12] utilized focal self-attention for capturing fine-grained details of long-range spatial interactions.

Mamba. Since the introduction of Mamba, a number of efforts have been proposed to leverage its capability for vision applications. Specifically, Vim [3] proposed to use a bidirectional SSM formulation, with the same Mamba formulation, in which tokens were processed in both forward and backward directions in order to capture more global context and improve spatial understanding. However, bidirectional encoding increases the computational load which can slow down training and inference times. In addition, combining information from multiple directions effectively to form a coherent global understanding is challenging as some global context may be lost in the process. As opposed to Vim, our proposed MambaVision uses a single forward pass with a redesigned Mamba block that can capture both short and long-range information and outperform it significantly both in terms of ImageNet Top-1 accuracy and throughput.

EfficientVMamba [4] proposed an atrous-based selective scan with a skip sampling approach to efficiently extract global spatial dependencies. EfficientVMamba also uses a hierarchical architecture, composed of SSM and CNN-based blocks, in which SSMs are used for larger input resolutions to better capture global context while CNNs are used for lower resolutions. In contrast to EfficientVMamba, MambaVision uses CNNs in higher resolutions for faster feature extraction while using both SSMs and self-attention in lower resolution to capture fine-grained details in both short and long-range spatial dependencies. Our proposed MambaVision also outperforms EfficientVMamba by a significant margin in terms of both Top-1 accuracy and image throughput.

In addition, VMamba [13] introduced a generic Mamba-based vision backbone with a Cross-Scan Module (CSM) which facilitates 1D selective scan with an enlarged global receptive field. Specifically, the CSM modules adopt a four-way selective scan methodology (*i.e.* upper-left and lower-right to opposite directions) to integrate information from all surrounding tokens and capture more global context. In addition, VMamba makes architectural changes such as using depth-wise convolutions and a hierarchical multi-resolution structure. Although the design of the CSM module is more suited for vision tasks, the receptive field is still limited by the cross-scan paths. In comparison to VMamba, the design of our proposed MambaVision mixer is simpler and can capture both short and long-range dependencies. MambaVision also uses CNN-based layer for fast feature extraction as opposed to VMamba which uses the same block structures in all stages. Furthermore, the MambaVision models outperform VMamba counterparts while having significantly higher image throughput.

3 Methodology

3.1 Macro Architecture

In this section, we introduce MambaVision which is our proposed novel architecture with SOTA performance on ImageNet-1K dataset. As illustrated in Fig. 2, MambaVision has a hierarchical architecture consisting of 4 different stages. The first two stages consist of CNN-based layers for fast feature extraction at higher input resolutions, while stage 3 and 4 include the proposed MambaVision and Transformer blocks. Specifically, given an image of size $H \times W \times 3$, the input is first converted into overlapping patches with size $\frac{H}{4} \times \frac{W}{4} \times C$ and projected into a C dimensional embedding space by the stem which consists of two consecutive 3×3 CNN layers with stride of 2. The downsampler in between stages consists of a batch normalized 3×3 CNN layer with stride 2 which reduces the image resolution by half. Furthermore, the CNN blocks in stages 1 and 2 follow a generic residual block formulation according to the following

$$\begin{aligned} \hat{\mathbf{z}} &= \text{GELU}(\text{BN}(\text{Conv}_{3 \times 3}(\mathbf{z}))), \\ \mathbf{z} &= \text{BN}(\text{Conv}_{3 \times 3}(\hat{\mathbf{z}})) + \mathbf{z}, \end{aligned} \tag{1}$$

GELU and BN denote Gaussian Error Linear Unit activation function [14] and batch normalization [15], respectively.

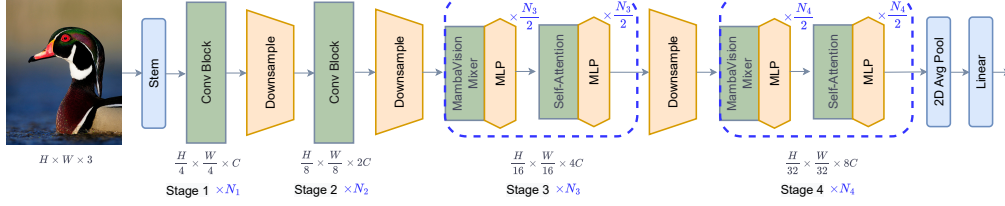


Figure 2 – The architecture of hierarchical MambaVision models. The first two stages use residual convolutional blocks for fast feature extraction. Stage 3 and 4 employ both MambaVision and Transformer blocks. Specifically, given N layers, we use $\frac{N}{2}$ MambaVision and MLP blocks which are followed by additional $\frac{N}{2}$ Transformer and MLP blocks. The Transformer blocks in final layers allow for recovering lost global context and capture long-range spatial dependencies.

3.2 Micro Architecture

In this section, we first revisit the preliminaries of Mamba and SSMS. We then present the micro design of the architecture in stages 3 and 4 and discuss MambaVision formulation in more details.

3.2.1 Mamba Preliminaries

Mamba is an extension of Structured state space models (S4) which is capable of transforming a 1D continuous input $x(t) \in \mathbb{R}$ to $y(t) \in \mathbb{R}$ via a learnable hidden state $h(t) \in \mathbb{R}^M$ with parameters $\mathbf{A} \in \mathbb{R}^{M \times M}$, $\mathbf{B} \in \mathbb{R}^{1 \times M}$ and $\mathbf{C} \in \mathbb{R}^{1 \times M}$ according to

$$\begin{aligned} h'(t) &= \mathbf{A}h(t) + \mathbf{B}x(t), \\ y(t) &= \mathbf{C}h(t), \end{aligned} \quad (2)$$

Discretization The continuous parameters \mathbf{A} , \mathbf{B} and \mathbf{C} in the above formulation are further converted into discrete parameters for better computational efficiency [16]. Specifically, assuming a timescale Δ , a zero-order hold rule can be applied to obtain discrete parameters $\bar{\mathbf{A}} \in \mathbb{R}^{M \times M}$, $\bar{\mathbf{B}} \in \mathbb{R}^{1 \times M}$ and $\bar{\mathbf{C}} \in \mathbb{R}^{1 \times M}$ according to

$$\begin{aligned} \bar{\mathbf{A}} &= \exp(\Delta \mathbf{A}), \\ \bar{\mathbf{B}} &= (\Delta \mathbf{A})^{-1}(\exp(\Delta \mathbf{A}) - \mathbf{I}) \cdot (\Delta \mathbf{B}), \\ \bar{\mathbf{C}} &= \mathbf{C}, \end{aligned} \quad (3)$$

The Eq. 2 can then be expressed with discrete parameters as

$$\begin{aligned} h(t) &= \bar{\mathbf{A}}h(t-1) + \bar{\mathbf{B}}x(t), \\ y(t) &= \bar{\mathbf{C}}h(t), \end{aligned} \quad (4)$$

In addition, for an input sequence with size T , a global convolution with kernel $\bar{\mathbf{K}}$ can be applied for computing the output of Eq. 4 as in the following

$$\begin{aligned} \bar{\mathbf{K}} &= (\bar{\mathbf{C}}\bar{\mathbf{B}}, \bar{\mathbf{C}}\bar{\mathbf{A}}\bar{\mathbf{B}}, \dots, \bar{\mathbf{C}}\bar{\mathbf{A}}^{T-1}\bar{\mathbf{B}}) \\ \mathbf{y} &= \mathbf{x} * \bar{\mathbf{K}}, \end{aligned} \quad (5)$$

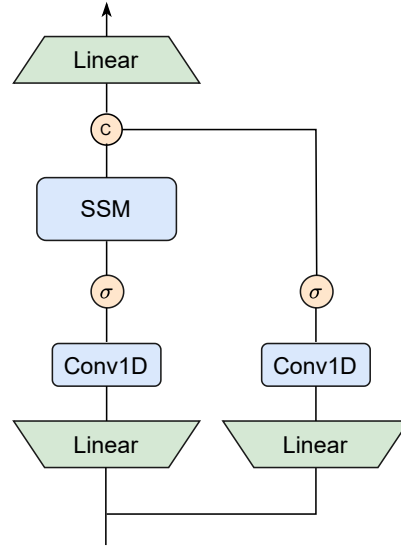


Figure 3 – Architecture of MambaVision block. In addition to replacing causal Conv layer with their regular counterparts, we create a symmetric path without SSM as a token mixer to enhance the modeling of global context.

Algorithm 1 PyTorch-like pseudo-code for MambaVision mixer

```

import torch
import math
import torch.nn as nn
import torch.nn.functional as F
from einops import rearrange, repeat

class MambaVisionMixer(nn.Module):
    def __init__(self, dim, d_state=16, kernel_size=3):
        super().__init__()
        self.d_state = d_state
        self.dt_rank = math.ceil(dim / 16)
        self.in_proj = nn.Linear(self.d_model, self.d_inner)
        self.x_proj = nn.Linear(dim//2, self.dt_rank + self.d_state * 2)
        self.conv1d_x = nn.Conv1d(dim//2, dim//2, kernel_size=kernel_size, padding='same', groups=dim//2)
        self.conv1d_z = nn.Conv1d(dim//2, dim//2, kernel_size=kernel_size, padding='same', groups=dim//2)
        self.dt_proj = nn.Linear(self.dt_rank, dim//2)
        dt = torch.exp(torch.rand(self.dim//2) * (math.log(dt_max) - math.log(dt_min)) + math.log(dt_min))
        A_log = torch.log(repeat(torch.arange(1, self.d_state + 1), n -> d n, d=dim//2))
        self.A_log = nn.Parameter(A_log)
        self.D = nn.Parameter(torch.ones(dim//2))
        self.out_proj = nn.Linear(dim, dim)

    def forward(self, hidden_states):
        xz = rearrange(self.in_proj(hidden_states), b l d -> b d l)
        x, z = xz.chunk(2, dim=1)
        A = -torch.exp(self.A_log)
        x = F.silu(self.conv1d_x(x))
        z = F.silu(self.conv1d_z(z))
        seqlen = hidden_states.shape[1]
        x_dbl = self.x_proj(rearrange(x, b d l -> (b l) d))
        dt, B, C = torch.split(x_dbl, [self.dt_rank, self.d_state, self.d_state], dim=-1)
        dt = rearrange(self.dt_proj(dt), (b l) d -> b d l, l=seqlen)
        B = rearrange(B, (b l) dstate -> b dstate l, l=seqlen)
        C = rearrange(C, (b l) dstate -> b dstate l, l=seqlen)
        x_ssm = selective_scan_fn(x, dt, A, B, C, D)
        hidden_states = rearrange(torch.cat([x_ssm, z], dim=1), b d l -> b l d)
        return self.out_proj(hidden_states)

```

Selectivity Mamba further extends the S4 formulation by introducing a selection mechanism which allows for input-dependant sequence processing. This allows the model’s parameters B , C and Δ to be adjusted dynamically according to the inputs and filter out irrelevant information. Further discretization details are provided in [2].

3.2.2 Layer Architecture

Assuming an input $X \in \mathbb{R}^{T \times C}$ with sequence length T with embedding dimension C , the output of layer n in stages 3 and 4 can be computed as in

$$\begin{aligned}
 \hat{X}^n &= \text{Mixer}(\text{Norm}(X^{n-1})) + X^{n-1} \\
 X^n &= \text{MLP}(\text{Norm}(\hat{X}^n)) + \hat{X}^n,
 \end{aligned}
 \tag{6}$$

Norm and Mixer denote the choices of layer normalization and token mixing blocks, respectively. Without loss of generality, Layer Normalization is used for Norm. Given N layers, the first $\frac{N}{2}$ layers employ MambaVision mixer blocks while the remaining $\frac{N}{2}$ layers employ self-attention. We describe the details of each mixer in the following.

MambaVision Mixer As shown in Fig. 3, we redesigned the original Mamba mixer to make it more suitable for vision tasks. First, we propose to replace the causal convolution with regular convolution, since it limits the influence to one direction, which is unnecessary and restrictive for vision tasks. In addition, we added a symmetric branch without SSM, consisting of an additional convolution and SiLU activation, to compensate for any content lost due to the sequential constraints of SSMs. We then concatenate the output of both branches and project it via a final linear layer. This combination ensures that the final feature representation incorporates both the sequential and spatial information, leveraging the strengths of both branches. We note that the output of each branch is projected into an embedding space with size $\frac{C}{2}$ (i.e. half the size of original embedding dimension) to maintain similar number of parameters to the original block design. Given an input X_{in} , the output of MambaVision

mixer X_{out} is computed according to

$$\begin{aligned} X_1 &= \text{Scan}(\sigma(\text{Conv}(\text{Linear}(C, \frac{C}{2})(X_{in})))) \\ X_2 &= \sigma(\text{Conv}(\text{Linear}(C, \frac{C}{2})(X_{in}))) \\ X_{out} &= \text{Linear}(\frac{C}{2}, C)(\text{Concat}(X_1, X_2)), \end{aligned} \quad (7)$$

$\text{Linear}(C_{in}, C_{out})(\cdot)$ denotes a linear layer with C_{in} and C_{out} as input and output embedding dimensions, Scan is the selective scan operation as in [2] and σ is the activation function for which Sigmoid Linear Unit (SiLU) [17] is used. In addition, Conv and Concat represent 1D convolution and concatenation operations. In Algorithm 1, we present a PyTorch-like pseudo-code for MambaVision mixer. In general, our proposed modification leads to richer feature representations, better generalization, and improved performance on computer vision tasks. We have also experimentally validated the effectiveness of each of our design choices in Sec.

Self-attention We use a generic multihead self-attention mechanism in accordance to

$$\text{Attention}(Q, K, V) = \text{Softmax}\left(\frac{QK^T}{\sqrt{d_h}}\right)V. \quad (8)$$

Q, K, V denote query, key and value respectively and d_h is the number of attention heads. Without loss of generality, the attention formulation which can be computed in a windowed manner similar to previous efforts [10, 18]

4 Experiments

Image classification experiments are conducted on ImageNet-1K dataset [19]. We followed the standard training recipe of previous efforts [10, 12, 29] to allow for a comparable analysis for performance of different models. Specifically, all models have been trained for 300 epochs with a cosine decay scheduler which uses an additional 20 epochs for warmup and cooldown phases, respectively. Furthermore, we use the LAMB optimizer [30] with global batch size of 4096, an initial learning rate of 0.005 and weight decay of 0.05. We note that using the LAMB optimizer resulted in better results compared to traditional AdamW [31], particularly due to its robustness to higher learning rates. We used 32 A100 GPUs for classification tasks.

To evaluate the performance of downstream tasks, we used our pre-trained models as backbones for object detection and instance segmentation and semantic segmentation tasks and used the MS COCO dataset [32] and ADE20K dataset [33], respectively. Specifically, for object detection and instance segmentation, we used Mask-RCNN [34] head with hyperparameters such as $\times 3$ LR schedule with an initial learning rate of 0.0001, a batch size of 16 and weight decay of 0.05. For semantic segmentation, we used an UperNet network [35] head with Adam-W [31] optimizer, an initial learning rate of $6e-5$ and a global batch size of 16. We used 8 A100 GPUs for all downstream tasks.

5 Results

5.1 Image classification

In Table 1, we present the ImageNet-1K classification results. Specifically, we compare against different families of models such as Conv-based, Transformer-based, Conv-Transformer and Mamba-based and demonstrate that our model outperforms the previous efforts by a large margin, considering ImageNet Top-1 accuracy and image throughput. For instance, when compared to popular models such as ConvNeXt and Swin Transformers, MambaVision-B (84.2%) ConvNeXt-B (83.8%) and Swin-B (83.5%), respectively, while also having significantly better image throughput. We observe similar trends in comparison to Mamba-based models. Specifically, MambaVision-B (84.2%) outperforms VMamba-B (83.9%) despite having considerably higher image throughput. We would also like to note that although our main design goal has been to the accuracy and throughput tradeoff, the MambaVision model variants have much lower FLOPs when compared to similarly-sized counterparts. For instance, MambaVision-B has 56% less GFLOPs than MaxViT-B.

Table 1 – Classification benchmarks on **ImageNet-1K** [19] dataset. Image throughput is computed on A100 GPU with a batch size of 128.

Model	Image Size (Px)	#Param (M)	FLOPs (G)	Throughput (Img/Sec)	Top-1 (%)
Conv-Based					
ConvNeXt-T [20]	224	28.6	4.5	3196	82.0
ConvNeXt-S [20]	224	50.2	8.7	2008	83.1
ConvNeXt-B [20]	224	88.6	15.4	1485	83.8
RegNetY-040 [21]	288	20.6	6.6	3227	83.0
EfficientNetV2-S [22]	384	21.5	8.0	1735	83.9
Transformer-Based					
Swin-T [10]	224	28.3	4.4	2758	81.3
Swin-S [10]	224	49.6	8.5	1720	83.2
Swin-B [10]	224	88.0	15.4	1245	83.5
SwinV2-T [18]	256	28.3	4.4	1674	81.8
SwinV2-S [18]	256	49.7	8.5	1043	83.8
SwinV2-B [18]	256	87.9	15.1	535	84.6
TNT-S [23]	224	23.8	4.8	1478	81.5
Twins-S [11]	224	24.1	2.8	3596	81.7
Twins-B [11]	224	56.1	8.3	1926	83.1
DeiT3-L	224	304.4	59.7	535	84.8
PoolFormer-M58 [24]	224	73.5	11.6	884	82.4
Conv-Transformer					
CoaT-Lite-S [25]	224	19.8	4.1	2269	82.3
CrossViT-B [26]	240	105.0	20.1	1321	82.2
NextViT-small	224	31.7	5.8	3834	82.5
NextViT-B	224	44.8	8.3	2926	83.2
MaxViT-B [27]	224	120.0	23.4	507	84.9
MaxViT-L [27]	224	212.0	43.9	376	85.1
FasterViT-1 [28]	224	53.4	5.3	4188	83.2
FasterViT-2 [28]	224	75.9	8.7	3161	84.2
FasterViT-3 [28]	224	159.5	18.2	1780	84.9
Mamba-Based					
Vim-T [3]	224	7.0	-	3957	76.1
Vim-S [3]	224	26.0	-	1974	80.5
EfficientVMamba-T [4]	224	6.0	0.8	2904	76.5
EfficientVMamba-S [4]	224	11.0	1.3	1610	78.7
EfficientVMamba-B [4]	224	33.0	4.0	1482	81.8
VMamba-T [13]	224	30.0	4.9	1282	82.6
VMamba-S [13]	224	50.0	8.7	843	83.6
VMamba-B [13]	224	89.0	15.4	645	83.9
MambaVision					
Mamba Vision-T	224	31.8	4.4	6298	82.3
Mamba Vision-T2	224	35.1	5.1	5990	82.7
Mamba Vision-S	224	50.1	7.5	4700	83.3
Mamba Vision-B	224	97.7	15.0	3670	84.2
Mamba Vision-L	224	227.9	34.9	2190	85.0
Mamba Vision-L2	224	241.5	37.5	1021	85.3

5.2 Object Detection and Segmentation

We present object detection and instance segmentation results on MS COCO dataset [32] in Table 2. Specifically, we have trained models with different detection sizes to further validate the effectiveness of MambaVision under different scenarios. We also note that our goal is not to achieve SOTA in these tasks but to compare the performance of our backbone with comparably-sized popular vision backbones and validate its effectiveness. With a simple Mask-RCNN detection head,

Backbone	Param (M)	FLOPs (G)	AP ^{box}	AP ₅₀ ^{box}	AP ₇₅ ^{box}	AP ^{mask}	AP ₅₀ ^{mask}	AP ₇₅ ^{mask}
Mask-RCNN 3× schedule								
Swin-T [10]	48	267	46.0	68.1	50.3	41.6	65.1	44.9
ConvNeXt-T [20]	48	262	46.2	67.9	50.8	41.7	65.0	44.9
MambaVision-T	48	255	46.4	68.3	51.0	41.8	65.4	45.0
Cascade Mask-RCNN 3× schedule								
DeiT-Small/16 [6]	80	889	48.0	67.2	51.7	41.4	64.2	44.3
ResNet-50 [36]	82	739	46.3	64.3	50.5	40.1	61.7	43.4
Swin-T [10]	86	745	50.4	69.2	54.7	43.7	66.6	47.3
ConvNeXt-T [20]	86	741	50.4	69.1	54.8	43.7	66.5	47.3
MambaVision-T	86	740	51.0	69.9	55.6	44.3	67.2	48.1
X101-32 [37]	101	819	48.1	66.5	52.4	41.6	63.9	45.2
Swin-S [10]	107	838	51.9	70.7	56.3	45.0	68.2	48.8
ConvNeXt-S [20]	108	827	51.9	70.8	56.5	45.0	68.4	49.1
MambaVision-S	108	828	52.1	70.9	56.7	45.2	68.4	49.1
X101-64 [37]	140	972	48.3	66.4	52.3	41.7	64.0	45.1
Swin-B [10]	145	982	51.9	70.5	56.4	45.0	68.1	48.9
ConvNeXt-B [20]	146	964	52.7	71.3	57.2	45.6	68.9	49.5
MambaVision-B	145	964	52.8	71.6	57.2	45.7	69.0	49.5

Table 2 – Object detection and instance segmentation results with Mask R-CNN and Cascade Mask R-CNN networks using MS COCO dataset [32].

our pretrained MambaVision-T backbone achieves 46.4 and 41.8 in terms of box AP and mask AP, respectively, outperforming both ConvNeXt-T [20] and Swin-T [10] models. With a Cascade Mask-RCNN network, MambaVision-T, MambaVision-S and MambaVision-B outperform the competing counterparts. Specifically, MambaVision models outperform ConvNeXt-T by +0.6 and 0.6, ConvNeXt-S by +0.2 and 0.2 and ConvNeXt-B by +0.1 and 0.1 in terms of box AP and mask AP, respectively. Similarly, MambaVision outperforms Swin-T by +0.6 and 0.6, Swin-S by +0.1 and 0.2 and Swin-B by +0.9 and 0.7 in terms of box AP and mask AP, respectively.

We present semantic segmentation benchmarks on the ADE20K dataset [33] in Table 3. For these experiments, we used a UPerNet [35] to be comparable to other models. We observe that MambaVision models outperform similarly-sized competing models for different variants. For instance, MambaVision-T, MambaVision-S and MambaVision-B outperform Swin-T, Swin-S and Swin-B by +0.6, +0.6 and +1.0 in terms of mIoU. Despite the fact that we did not perform extensive optimizations for hyper-parameter tuning of downstream tasks, these results demonstrate the feasibility of MambaVision as a promising backbone for different vision tasks, especially in high-resolution settings.

Backbone	Param (M)	FLOPs (G)	mIoU
DeiT-Small/16 [6]	52	1099	44.0
Swin-T [10]	60	945	44.5
ResNet-101 [36]	86	1029	44.9
Focal-T [12]	62	998	45.8
Twins-SVT-S [11]	55	-	46.2
MambaVision-T	55	945	46.6
Swin-S [10]	81	1038	47.6
Twins-SVT-B [11]	89	-	47.7
Focal-S [12]	85	1130	48.0
MambaVision-S	84	1135	48.2
Swin-B [10]	121	1188	48.1
Twins-SVT-L [11]	133	-	48.8
Focal-B [12]	126	1354	49.0
MambaVision-B	126	1342	49.1

Table 3 – Semantic segmentation results with UperNet [35] networks using ADE20K dataset. For all models, a crop size of 512×512 is used.

5.3 Ablation

Design of Token Mixer In this section, we perform a comprehensive ablation study for a systematic design of MambaVision token mixer. Our goal is to modify the existing Mamba block for computer vision tasks and we evaluate the performance for different tasks such as classification, object detection and instance segmentation and semantic segmentation. All experiments follow a model similar to the architecture layout of the MambaVision-T model as the basis.

As shown in Table 4, we start by using the original Mamba formulation with the causal conv layer in the SSM branch (*i.e.* conv1) and without the additional conv layer in our proposed symmetric branch (*i.e.* conv2). As expected, this formulation achieves a suboptimal performance with a Top-1 accuracy of 80.9% (−1.8%), box AP and mask AP of 44.8 (−1.6) and 40.2 (−1.6) and mIoU of 44.2% (−1.4). We then replace the causal conv of SSM branch (*i.e.* conv1) with a regular conv layer and observe improvements in terms of all metrics due to this change. Furthermore, we add conv2 layer but use the same gating mechanism of Mamba instead of concatenation. This change improves the performance and leads to a Top-1 accuracy of 81.3%, box AP and mask AP of 45.3 and 41.0 and mIoU of 45.7%. Finally, adding concatenation considerably improves the performance in all metrics by +1.0%, +1.1, +0.8 and +0.9 in terms of ImageNet Top-1, box AP and mask AP for MS COCO and mIoU for ADE20K dataset. Hence, this validates our hypothesis that concatenating the outputs from both branches (*i.e.* SSM and non-SSM) leads to learning richer feature representation and enhancing global context understanding.

	ImageNet	COCO		ADE20k
	top-1	AP ^{box}	AP ^{mask}	mIoU
causal conv1 - w/o conv2	80.5	44.8	40.4	44.2
conv1 - w/o conv2	80.9	45.0	40.8	44.7
conv1 - conv2 - w/o concat	81.3	45.3	41.0	45.7
conv1 - conv2 - concat	82.3	46.4	41.8	46.6

Table 4 – Systematic design of MambaVision token mixer. w/o and concat refer "without" and concatenation. conv1 and conv2 denote the conv operations in the SSM and additional symmetric branch as shown in Fig. 3. The performance is evaluated on ImageNet-1K, MS COCO and ADE20K dataset for classification, object detection and instance segmentation and semantic segmentation, respectively.

Hybrid Pattern In this section, we comprehensively study the effect of different hybrid integration patterns for self-attention and MambaVision token mixers. For all experiments, the architecture follows MambaVision-T layout with and we keep the models iso-parameter for fair comparison. The patterns are utilized for stages 3 and 4 with hybrid functionality. We begin our study by using a random pattern and achieve a suboptimal Top-1 accuracy of 81.3%. This confirms our previous intuition that simply using self-attention without a specific pattern may not be effective. We then utilize the self-attention blocks in the first $N/2$ layers for each stage, with N representing the total number of stage layers, and observe an improvement of +0.2% (81.5%) in Top-1 accuracy. However, using a mixed layer pattern of self-attention/MambaVision mixers blocks slightly reduces the accuracy by −0.1% (81.4%). Conversely, reversing the order of mixed layers by using MambaVision/self-attention improves the performance and archives a Top-1 accuracy of (81.6%). We then utilize self-attention blocks in only the last $N/4$ layers of each stage and observe an immediate improvement of +0.3% (81.9%) in the accuracy. This validates our hypothesis that using self-attention blocks in the final layers of each stage is an effective design. However, its representation learning capability needs to be tuned with respect to MambaVision layers. Increasing the number of self-attention blocks to $N/2$ last layers of each stage achieves the best performance of 82.3%.

Model	Top-1
Random	81.3
First $N/2$ layers (SSSSMMMM)	81.5
Mixed layers-1 (SMSMSMSM)	81.4
Mixed layers-2 (MSMSMSMS)	81.6
Last $N/4$ layers (MMMMMMSS)	81.9
Last $N/2$ layers (MMMMSSSS)	82.3

Table 5 – Ablation study of on the effectiveness of different hybrid integration patterns using ImageNet-1K dataset. We use the specified patterns for stages 3 and 4. However, only stage 3 ($N=8$) patterns have been shown in the table for illustration purposes. S and M denote self-attention and MambaVision token mixer blocks, respectively.

6 Conclusion

In this work, we introduced MambaVision which is the first Mamba-Transformer hybrid backbone specifically tailored for vision applications. We proposed re-design of Mamba formulation to enhance global context representation learning capability and presented a comprehensive study of hybrid design integration patterns. MambaVision achieves a new SOTA Pareto front in terms of Top-1 accuracy and image throughput, surpassing Transformer and Mamba-based models by a significant margin. We hope these findings could be the foundation for a new class of hybrid vision models.

References

- [1] Ashish Vaswani, Noam Shazeer, Niki Parmar, Jakob Uszkoreit, Llion Jones, Aidan N Gomez, Łukasz Kaiser, and Illia Polosukhin. Attention is all you need. In *Advances in neural information processing systems*, pages 5998–6008, 2017.
- [2] Albert Gu and Tri Dao. Mamba: Linear-time sequence modeling with selective state spaces. *arXiv preprint arXiv:2312.00752*, 2023.
- [3] Lianghai Zhu, Bencheng Liao, Qian Zhang, Xinlong Wang, Wenyu Liu, and Xinggang Wang. Vision mamba: Efficient visual representation learning with bidirectional state space model. *arXiv preprint arXiv:2401.09417*, 2024.
- [4] Xiaohuan Pei, Tao Huang, and Chang Xu. Efficientvmamba: Atrous selective scan for light weight visual mamba. *arXiv preprint arXiv:2403.09977*, 2024.
- [5] Alexey Dosovitskiy, Lucas Beyer, Alexander Kolesnikov, Dirk Weissenborn, Xiaohua Zhai, Thomas Unterthiner, Mostafa Dehghani, Matthias Minderer, Georg Heigold, Sylvain Gelly, et al. An image is worth 16x16 words: Transformers for image recognition at scale. In *International Conference on Learning Representations*, 2020.
- [6] Hugo Touvron, Matthieu Cord, Matthijs Douze, Francisco Massa, Alexandre Sablayrolles, and Hervé Jégou. Training data-efficient image transformers & distillation through attention. In *International Conference on Machine Learning*, pages 10347–10357. PMLR, 2021.
- [7] Benjamin Graham, Alaaeldin El-Nouby, Hugo Touvron, Pierre Stock, Armand Joulin, Hervé Jégou, and Matthijs Douze. Levit: a vision transformer in convnet’s clothing for faster inference. In *Proceedings of the IEEE/CVF International Conference on Computer Vision*, pages 12259–12269, 2021.
- [8] Alaaeldin Ali, Hugo Touvron, Mathilde Caron, Piotr Bojanowski, Matthijs Douze, Armand Joulin, Ivan Laptev, Natalia Neverova, Gabriel Synnaeve, Jakob Verbeek, et al. Xcit: Cross-covariance image transformers. *Advances in neural information processing systems*, 34, 2021.
- [9] Wenhai Wang, Enze Xie, Xiang Li, Deng-Ping Fan, Kaitao Song, Ding Liang, Tong Lu, Ping Luo, and Ling Shao. Pyramid vision transformer: A versatile backbone for dense prediction without convolutions. In *Proceedings of the IEEE/CVF International Conference on Computer Vision*, pages 568–578, 2021.
- [10] Ze Liu, Yutong Lin, Yue Cao, Han Hu, Yixuan Wei, Zheng Zhang, Stephen Lin, and Baining Guo. Swin transformer: Hierarchical vision transformer using shifted windows. In *Proceedings of the IEEE/CVF International Conference on Computer Vision*, pages 10012–10022, 2021.
- [11] Xiangxiang Chu, Zhi Tian, Yuqing Wang, Bo Zhang, Haibing Ren, Xiaolin Wei, Huaxia Xia, and Chunhua Shen. Twins: Revisiting the design of spatial attention in vision transformers. *Advances in Neural Information Processing Systems*, 34, 2021.
- [12] Jianwei Yang, Chunyuan Li, Pengchuan Zhang, Xiyang Dai, Bin Xiao, Lu Yuan, and Jianfeng Gao. Focal attention for long-range interactions in vision transformers. *Advances in Neural Information Processing Systems*, 34, 2021.
- [13] Yue Liu, Yunjie Tian, Yuzhong Zhao, Hongtian Yu, Lingxi Xie, Yaowei Wang, Qixiang Ye, and Yunfan Liu. Vmamba: Visual state space model. *arXiv preprint arXiv:2401.10166*, 2024.
- [14] Dan Hendrycks and Kevin Gimpel. Gaussian error linear units (gelus). *arXiv preprint arXiv:1606.08415*, 2016.
- [15] Sergey Ioffe and Christian Szegedy. Batch normalization: Accelerating deep network training by reducing internal covariate shift. In *International conference on machine learning*, pages 448–456. PMLR, 2015.
- [16] Albert Gu, Isys Johnson, Karan Goel, Khaled Saab, Tri Dao, Atri Rudra, and Christopher Ré. Combining recurrent, convolutional, and continuous-time models with linear state space layers. *Advances in neural information processing systems*, 34:572–585, 2021.

- [17] Stefan Elfving, Eiji Uchibe, and Kenji Doya. Sigmoid-weighted linear units for neural network function approximation in reinforcement learning. *Neural networks*, 107:3–11, 2018.
- [18] Ze Liu, Han Hu, Yutong Lin, Zhuliang Yao, Zhenda Xie, Yixuan Wei, Jia Ning, Yue Cao, Zheng Zhang, Li Dong, et al. Swin transformer v2: Scaling up capacity and resolution. In *Proceedings of the IEEE/CVF Conference on Computer Vision and Pattern Recognition*, pages 12009–12019, 2022.
- [19] Jia Deng, Wei Dong, Richard Socher, Li-Jia Li, Kai Li, and Li Fei-Fei. Imagenet: A large-scale hierarchical image database. In *2009 IEEE conference on computer vision and pattern recognition*, pages 248–255. Ieee, 2009.
- [20] Zhuang Liu, Hanzi Mao, Chao-Yuan Wu, Christoph Feichtenhofer, Trevor Darrell, and Saining Xie. A convnet for the 2020s. In *Proceedings of the IEEE/CVF Conference on Computer Vision and Pattern Recognition*, pages 11976–11986, 2022.
- [21] Ilija Radosavovic, Raj Prateek Kosaraju, Ross Girshick, Kaiming He, and Piotr Dollár. Designing network design spaces. In *Proceedings of the IEEE/CVF conference on computer vision and pattern recognition*, pages 10428–10436, 2020.
- [22] Mingxing Tan and Quoc Le. Efficientnetv2: Smaller models and faster training. In *International Conference on Machine Learning*, pages 10096–10106. PMLR, 2021.
- [23] Kai Han, An Xiao, Enhua Wu, Jianyuan Guo, Chunjing Xu, and Yunhe Wang. Transformer in transformer. *Advances in Neural Information Processing Systems*, 34:15908–15919, 2021.
- [24] Weihao Yu, Mi Luo, Pan Zhou, Chenyang Si, Yichen Zhou, Xinchao Wang, Jiashi Feng, and Shuicheng Yan. Metaformer is actually what you need for vision. In *Proceedings of the IEEE/CVF Conference on Computer Vision and Pattern Recognition*, pages 10819–10829, 2022.
- [25] Weijian Xu, Yifan Xu, Tyler Chang, and Zhuowen Tu. Co-scale conv-attentional image transformers. In *Proceedings of the IEEE/CVF International Conference on Computer Vision*, pages 9981–9990, 2021.
- [26] Chun-Fu Richard Chen, Quanfu Fan, and Rameswar Panda. Crossvit: Cross-attention multi-scale vision transformer for image classification. In *Proceedings of the IEEE/CVF international conference on computer vision*, pages 357–366, 2021.
- [27] Zhengzhong Tu, Hossein Talebi, Han Zhang, Feng Yang, Peyman Milanfar, Alan Bovik, and Yinxiao Li. Maxvit: Multi-axis vision transformer. In *Computer Vision—ECCV 2022: 17th European Conference, Tel Aviv, Israel, October 23–27, 2022, Proceedings, Part XXIV*, pages 459–479. Springer, 2022.
- [28] Ali Hatamizadeh, Greg Heinrich, Hongxu Yin, Andrew Tao, Jose M Alvarez, Jan Kautz, and Pavlo Molchanov. Fastvit: Fast vision transformers with hierarchical attention. *arXiv preprint arXiv:2306.06189*, 2023.
- [29] Ali Hatamizadeh, Hongxu Yin, Greg Heinrich, Jan Kautz, and Pavlo Molchanov. Global context vision transformers. In *International Conference on Machine Learning*, pages 12633–12646. PMLR, 2023.
- [30] Yang You, Jing Li, Sashank Reddi, Jonathan Hseu, Sanjiv Kumar, Srinadh Bhojanapalli, Xiaodan Song, James Demmel, Kurt Keutzer, and Cho-Jui Hsieh. Large batch optimization for deep learning: Training bert in 76 minutes. *arXiv preprint arXiv:1904.00962*, 2019.
- [31] Ilya Loshchilov and Frank Hutter. Decoupled weight decay regularization. *arXiv preprint arXiv:1711.05101*, 2017.
- [32] Tsung-Yi Lin, Michael Maire, Serge Belongie, James Hays, Pietro Perona, Deva Ramanan, Piotr Dollár, and C Lawrence Zitnick. Microsoft COCO: Common objects in context. In *ECCV*, 2014.

- [33] Bolei Zhou, Hang Zhao, Xavier Puig, Sanja Fidler, Adela Barriuso, and Antonio Torralba. Scene parsing through ade20k dataset. In *Proceedings of the IEEE conference on computer vision and pattern recognition*, pages 633–641, 2017.
- [34] Kaiming He, Georgia Gkioxari, Piotr Dollár, and Ross Girshick. Mask r-cnn. In *Proceedings of the IEEE international conference on computer vision*, pages 2961–2969, 2017.
- [35] Tete Xiao, Yingcheng Liu, Bolei Zhou, Yuning Jiang, and Jian Sun. Unified perceptual parsing for scene understanding. In *Proceedings of the European Conference on Computer Vision (ECCV)*, pages 418–434, 2018.
- [36] Kaiming He, Xiangyu Zhang, Shaoqing Ren, and Jian Sun. Deep residual learning for image recognition. In *Proceedings of the IEEE conference on computer vision and pattern recognition*, pages 770–778, 2016.
- [37] Saining Xie, Ross Girshick, Piotr Dollár, Zhuowen Tu, and Kaiming He. Aggregated residual transformations for deep neural networks. In *Proceedings of the IEEE conference on computer vision and pattern recognition*, pages 1492–1500, 2017.